Variedades invariantes y transporte en un sistema Tierra-Luna perturbado por el Sol

À. Jorba, B. Nicolás

Ddays, Lleida, 9 de Septiembre del 2021

UNIVERSITAT DE BARCELONA

TraX Stability and Transitions in Physical Processes

GOBIERNO DE ESPAÑA

MINISTERIO DE ECONOMÍA, INDUSTRIA Y COMPETITIVIDAD

AGENCIA ESTATAL DE INVESTIGACIÓN

Outline

Mathematical model

- Bicircular Problem (BCP)

Invariant objects near L_3 in the BCP model

- Dynamical equivalent
- Invariant tori and stability
- Invariant manifolds of invariant tori

Transport through L_3 in the BCP

- Entering and leaving orbits
- Lunar meteorites

Transport in a realistic model

- Change of coordinates
- Lunar meteorites

Capture of an asteroid

- High order parametrization of hyperbolic invariant manifolds

Restricted Three Body Problem (**RTBP**)

RTBP describes the movement of a massless particle subjected to the gravitational fields of two massive bodies (*primaries*) that revolve in circular motion around their barycentre.

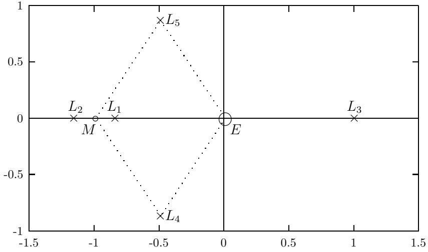

- We consider the **planar** case.
- $\mu = 0.012150582$ for the **Earth-Moon system**.
- Adimensional units such that gravitational constant is 1.
- **Synodic** reference frame.
- Earth is placed at $(\mu, 0)$, Moon at $(-1+\mu, 0)$.

$$H_{RTBP} = \frac{1}{2}(p_x^2 + p_y^2) + yp_x - xp_y - \frac{1-\mu}{r_{PE}} - \frac{\mu}{r_{PM}}$$

- Autonomous Hamiltonian.
- Energy is conserved.
- Five equilibrium points: L_1, L_2 and L_3 are unstable, while L_4 and L_5 are linearly stable.

Bicircular Problem (**BCP**)

BCP is a restricted 4-body problem, where the fourth body acts as a **time-periodic perturbation** of the RTBP.

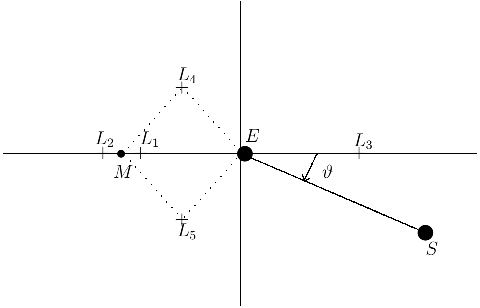

- Non-autonomous Hamiltonian**!!**
- Energy is not conserved.
- Five equilibrium points replaced by periodic orbits with the **period of the perturbation** (T).

$$H_{BCP} = H_{RTBP} + \hat{H}_{BPC}$$

where $\hat{H}_{BCP} = -\frac{m_s}{r_{PS}} - \frac{m_s}{a_s^2}(y \sin\vartheta - x \cos\vartheta)$, with $\vartheta = \omega_s t$ and $\omega_s = \frac{2\pi}{T}$.

Dynamical equivalent for L_3 in the BCP

- In the **RTBP**, L_3 equilibrium point of *centre* $\times$ *saddle* type.

Dynamical equivalent for L_3 in the BCP

- In the **RTBP**, L_3 equilibrium point of *centre* $\times$ *saddle* type.

Dynamical equivalent for L_3 in the BCP

- In the **RTBP**, L_3 equilibrium point of *centre* $\times$ *saddle* type. $\rightarrow$ Fam. of periodic orbits

Dynamical equivalent for L_3 in the BCP

- In the **RTBP**, L_3 equilibrium point of *centre* $\times$ *saddle* type.$\rightarrow$ Fam. of periodic orbits
- In the **BCP**, L_3 equilibrium point **becomes a periodic orbit of period** T, which is the dynamical equivalent of L_3 in the BCP:

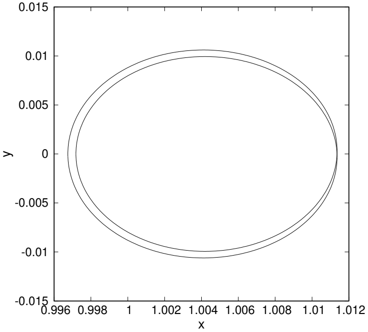

Its stability is again *centre* $\times$ *saddle*; unstable eigenvalue $\lambda_u \approx 3.37282$, ($\lambda_s = \lambda_u^{-1}$ due to the Hamiltonian structure).

Dynamical equivalent for L_3 in the BCP

- In the **RTBP**, L_3 equilibrium point of *centre* $\times$ *saddle* type. $\rightarrow$ Fam. of periodic orbits
- In the **BCP**, L_3 equilibrium point **becomes a periodic orbit of period** T, which is the dynamical equivalent of L_3 in the BCP: $\rightarrow$ Fam. of 2D quasi-periodic orbits

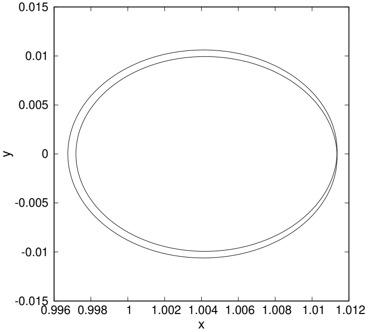

Its stability is again *centre* $\times$ *saddle*; unstable eigenvalue $\lambda_u \approx 3.37282$, ($\lambda_s = \lambda_u^{-1}$ due to the Hamiltonian structure).

Invariant tori and stability

Family of 2D invariant tori around L_3 dynamical substitute

- A family of **quasi-periodic orbits** emerges in the centre direction from L_3 periodic orbit.
- Each of the tori composing this family has **two frequencies**:
  - one comes from the family of Lyapunov periodic orbits of L_3 in the unperturbed system and it is different for each torus,
  - the other one is the frequency of the Sun, shared by them all.

Invariant tori and stability

Family of 2D invariant tori around L_3 dynamical substitute

- A family of **quasi-periodic orbits** emerges in the centre direction from L_3 periodic orbit.
- Each of the tori composing this family has **two frequencies**:
    - one comes from the family of Lyapunov periodic orbits of L_3 in the unperturbed system and it is different for each torus,
    - the other one is the frequency of the Sun, shared by them all.

Linear behaviour around them

- These invariant tori are **hyperbolic**.

Invariant tori and stability

Family of 2D invariant tori around L_3 dynamical substitute

- A family of **quasi-periodic orbits** emerges in the centre direction from L_3 periodic orbit.
- Each of the tori composing this family has **two frequencies**:
  - one comes from the family of Lyapunov periodic orbits of L_3 in the unperturbed system and it is different for each torus,
  - the other one is the frequency of the Sun, shared by them all.

Linear behaviour around them

- These invariant tori are **hyperbolic**.

Stable/Unstable invariant manifolds

- Each invariant manifold is **three dimensional**.

Stroboscopic map P

A Poincaré map corresponding to the period of the Sun, T, is applied to the flow, reducing one angular dimension. **In this map**:

- The dynamical substitute is seen as a fixed point.

Stroboscopic map P

A Poincaré map corresponding to the period of the Sun, T, is applied to the flow, reducing one angular dimension. **In this map**:

- The dynamical substitute is seen as a fixed point.
- The family of 2D invariant tori is seen as a family of 1D invariant curves.

Stroboscopic map P

A Poincaré map corresponding to the period of the Sun, T, is applied to the flow, reducing one angular dimension. **In this map**:

- The dynamical substitute is seen as a fixed point.
- The family of 2D invariant tori is seen as a family of 1D invariant curves.

Stroboscopic map P

A Poincaré map corresponding to the period of the Sun, T, is applied to the flow, reducing one angular dimension. **In this map**:

- The dynamical substitute is seen as a fixed point.
- The family of 2D invariant tori is seen as a family of 1D invariant curves.
  - Each curve $\varphi : \mathbb{T}^1 \mapsto \mathbb{R}^n$ with $n = 4$ is characterized by its **rotation number** ω and must satisfy the **invariance condition**:

$$P(\varphi(\theta)) = \varphi(\theta + \omega), \qquad \theta \in [0, 2\pi).$$

Stroboscopic map P

A Poincaré map corresponding to the period of the Sun, T, is applied to the flow, reducing one angular dimension. **In this map**:

- The dynamical substitute is seen as a fixed point.
- The family of 2D invariant tori is seen as a family of 1D invariant curves.
  - Each curve $\varphi : \mathbb{T}^1 \mapsto \mathbb{R}^n$ with $n = 4$ is characterized by its **rotation number** ω and must satisfy the **invariance condition**:

$$P(\varphi(\theta)) = \varphi(\theta + \omega), \qquad \theta \in [0, 2\pi).$$

  - We look for pairs of eigenvalue and eigenfunction (λ, ψ) that satisfy the **generalized eigenvalue problem** (GEV),

$$A(\theta)\psi(\theta) = \lambda T_\omega \psi(\theta),$$

where $A(\theta) = D_\varphi(P(\varphi(\theta)))$ and $T_\omega : \psi(\theta) \in C(\mathbb{T}^1, \mathbb{C}^4) \mapsto \psi(\theta + \omega) \in C(\mathbb{T}^1, \mathbb{C}^4)$.

Stroboscopic map P

A Poincaré map corresponding to the period of the Sun, T, is applied to the flow, reducing one angular dimension. **In this map**:

- The dynamical substitute is seen as a fixed point.
- The family of 2D invariant tori is seen as a family of 1D invariant curves.
  - Each curve $\varphi : \mathbb{T}^1 \mapsto \mathbb{R}^n$ with $n = 4$ is characterized by its **rotation number** ω and must satisfy the **invariance condition**:

$$P(\varphi(\theta)) = \varphi(\theta + \omega), \qquad \theta \in [0, 2\pi).$$

  - We look for pairs of eigenvalue and eigenfunction (λ, ψ) that satisfy the **generalized eigenvalue problem** (GEV),

$$A(\theta)\psi(\theta) = \lambda T_\omega \psi(\theta),$$

    where $A(\theta) = D_\varphi(P(\varphi(\theta)))$ and $T_\omega : \psi(\theta) \in C(\mathbb{T}^1, \mathbb{C}^4) \mapsto \psi(\theta + \omega) \in C(\mathbb{T}^1, \mathbb{C}^4)$.
- The 3D invariant manifolds are seen as two-dimensional.

Family of 1D invariant curves around L_3 in the map P

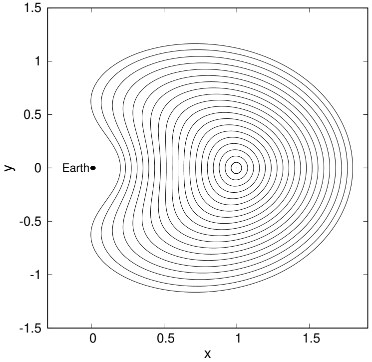

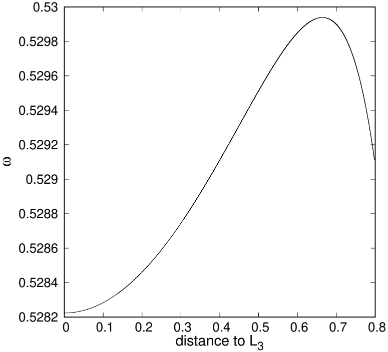

Family of 1D invariant curves around L_3 in the map P

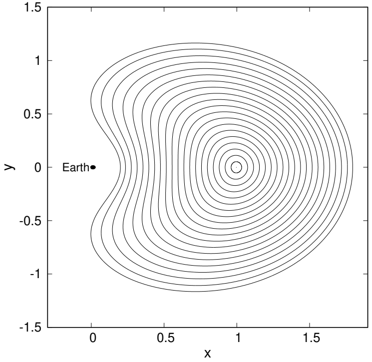

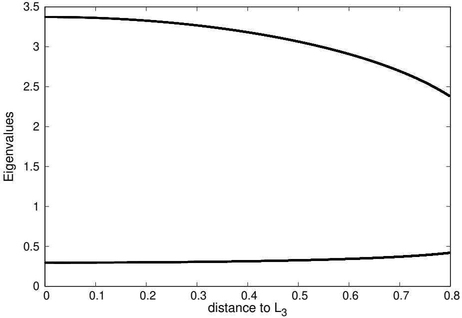

Linear approximation of invariant manifolds

We take an small displacement in the hyperbolic (**stable** or **unstable**) direction:

$$P(\varphi(\theta) + \sigma\psi_{s,u}(\theta)) = P(\varphi(\theta)) + \sigma D_\varphi(P(\varphi(\theta)))\psi_{s,u}(\theta) + \mathcal{O}(\sigma^2)$$

$$= \varphi(\theta + \omega) + \sigma\lambda_{s,u}\psi_{s,u}(\theta + \omega) + \mathcal{O}(\sigma^2).$$

Linear approximation of invariant manifolds

We take an small displacement in the hyperbolic (**stable** or **unstable**) direction:

$$P(\varphi(\theta)+\sigma\psi_{s,u}(\theta)) = P(\varphi(\theta)) + \sigma D_{\varphi}(P(\varphi(\theta)))\psi_{s,u}(\theta) + \mathcal{O}(\sigma^2)$$

$$= \varphi(\theta+\omega) + \sigma\lambda_{s,u}\psi_{s,u}(\theta+\omega) + \mathcal{O}(\sigma^2).$$

At every step of the integration we check if the orbits collide with some primary or if they leave the system.

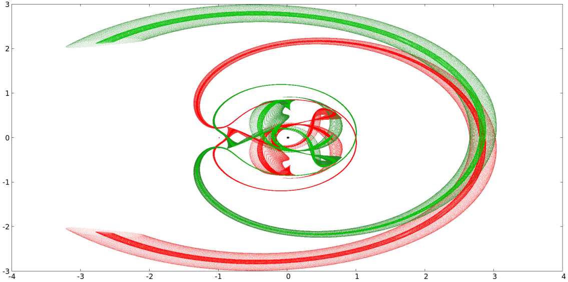

Stable (green) and unstable (red) invariant manifolds corresponding to two invariant curves, in the xy-plane.

Transport through L_3 in the BCP

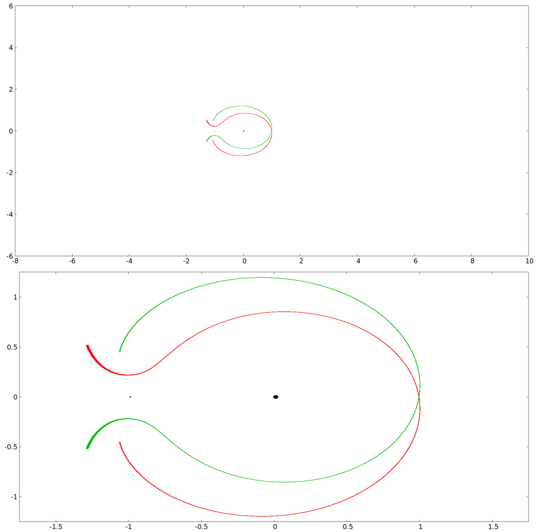

Transport through L_3 in the BCP

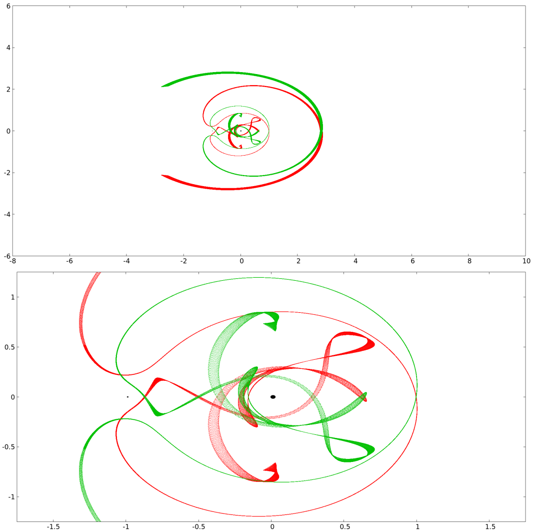

Transport through L_3 in the BCP

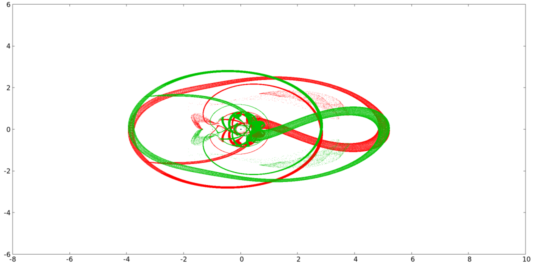

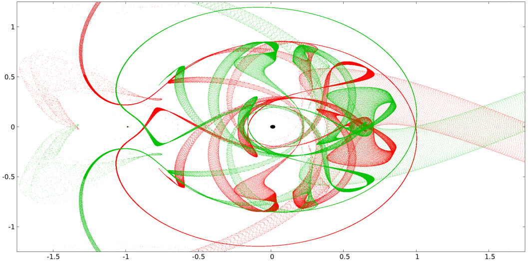

Transport through L_3 in the BCP

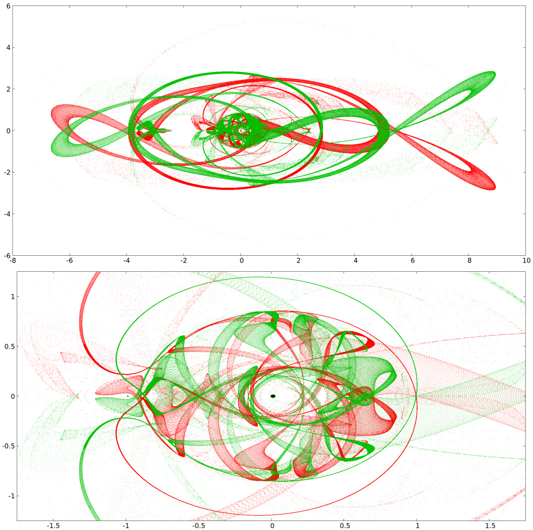

Transport through L_3 in the BCP

Fundamental cylinder

Fundamental region (the small "cylinder") used for globalizing the invariant manifolds, is defined by two parameters (θ, σ).

For example, the parametrization of the fundamental region of the **unstable manifold** for an invariant curve φ is perfomed as:

$$(\theta, \sigma) \in [0, 2\pi] \times [\sigma_0, \lambda_u \sigma_0] \mapsto \varphi(\theta) + \sigma \psi_u(\theta),$$

for $\sigma_0 > 0$ and $\sigma_0 < 0$.

With these two parameters we define a **mesh of initial points** of the four invariant manifolds for an invariant curve and **colored them according to their fate**.

Transport through L_3 in the BCP

Color (fate): Purple (Earth), red (Moon), yellow (leaving the system), or black (neither).

Invariant torus at 0.03335 **from** $\mathbf{L_3}$**.**

Unstable manifold, Left/right, taking positive/negative displacement.

Stable manifold, Left/right, taking positive/negative displacement.

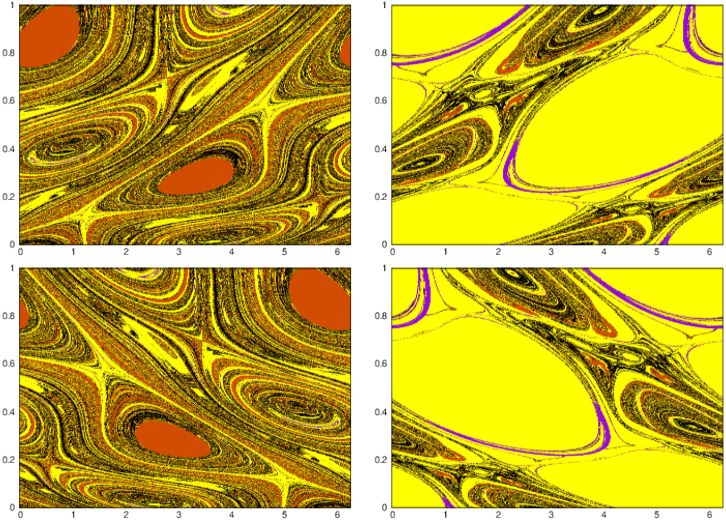

Transport through L_3 in the BCP

Color (fate): Purple (Earth), red (Moon), yellow (leaving the system), or black (neither).

Unstable manifolds of invariant tori at 0.19607 from L_3.

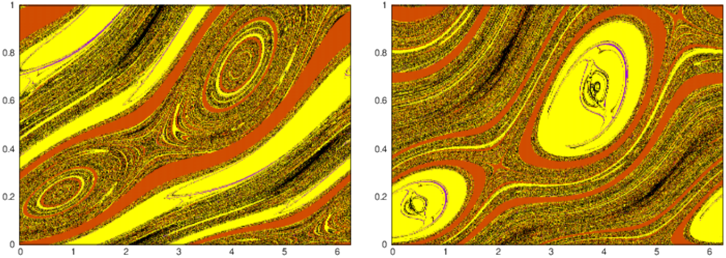

Transport through L_3 in the BCP

Color (fate): Purple (Earth), red (Moon), yellow (leaving the system), or black (neither).

Unstable manifolds of invariant tori at 0.19607 from L_3.

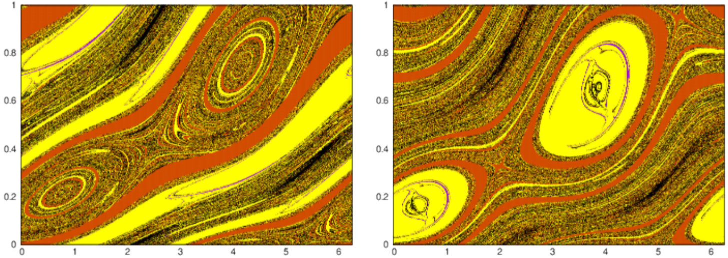

Unstable manifolds of invariant tori at 0.30902 from L_3.

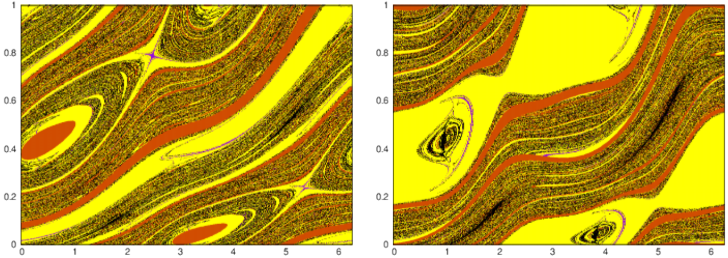

Transport through L_3 in the BCP

Color (fate): Purple (Earth), red (Moon), yellow (leaving the system), or black (neither).

Unstable manifolds
of invariant tori
at 0.57020 from L_3.

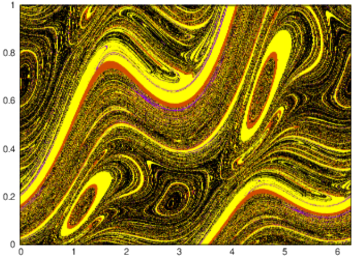

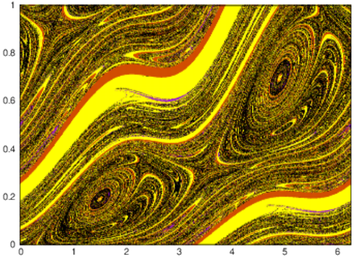

Transport through L_3 in the BCP

Color (fate): Purple (Earth), red (Moon), yellow (leaving the system), or black (neither).

Unstable manifolds of invariant tori at 0.57020 from L_3.

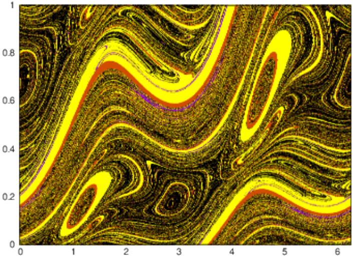

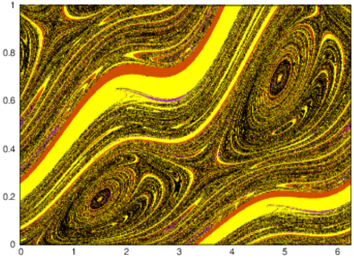

Unstable manifolds of invariant tori at 0.74214 from L_3.

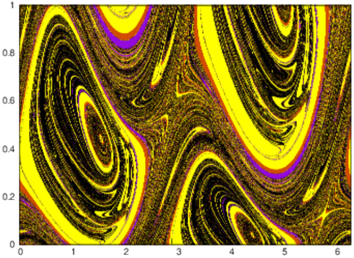

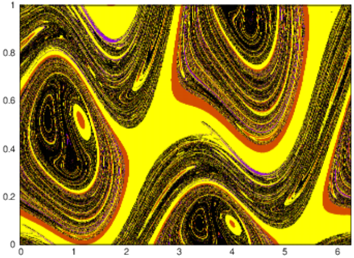

Entering and leaving orbits

- The trajectories that leave and enter in the Earth-Moon system may give us an insight about NEOs (**Near Earth Objects**) behaviour.
- Entering/Leaving orbits have been defined as those orbits that get at some distance far away from the Earth-Moon barycenter, since they are considered to be captured by solar gravitatory field.
- Orbital Elements (OE) with respect to the Sun have been computed.

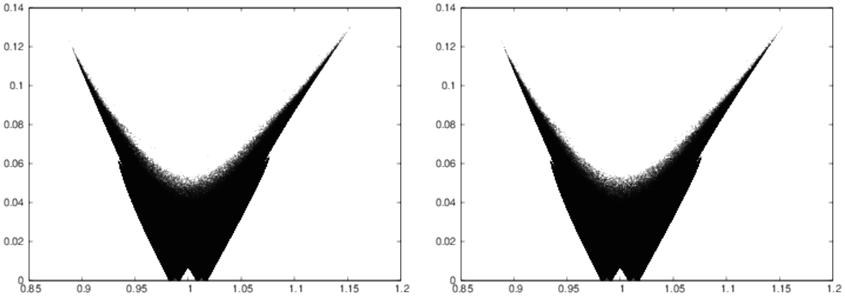

Eccentricity vs semimajor axis (in astronomical units). Left, OE for orbits entering in the system, right, OE for orbits leaving it.

Lunar meteorites

- Moon surface suffers several impacts every year.
- If the velocity of the crater ejecta is higher than the lunar escape velocity (≈ 2.38 km/s), they get free from the Moon gravity and become lunar meteorites.
- Some lunar meteorites are found on the Earth.

Lunar meteorites

- Moon surface suffers several impacts every year.
- If the velocity of the crater ejecta is higher than the lunar escape velocity (≈ 2.38 km/s), they get free from the Moon gravity and become lunar meteorites.
- Some lunar meteorites are found on the Earth.

Stable invariant manifolds that goes from the **Moon** to L_3 vicinity and **connect** with **unstable** invariant manifolds that leave this surroundings towards the **Earth**, may explain the travel that lunar meteorites make to reach our planet.

Lunar meteorites

Several of these connections have been found for the BCP:

- No preferred point on the Moon (origin) neither on the Earth (destination) was found.
- Also, these connections happen at any time (no preferred $\vartheta = \omega_s t$).
- Range of velocities for leaving the Moon surface is $[2.25, 3.38]$ km/s.
- Range of velocities when they reach the Earth surface (neglecting atmosphere effects) is $[11.00, 11.31]$ km/s.

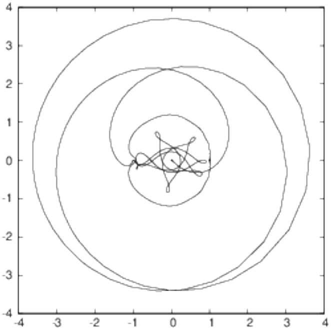

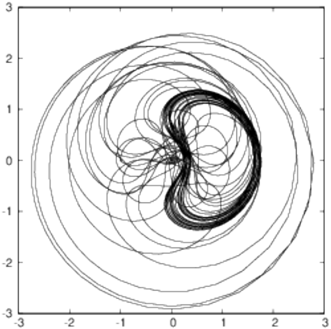

Lunar meteorites

Origin of these trajectories: intersection of the stable invariant manifolds of L_3 with the Moon's surface.

Lunar meteorites

Origin of these trajectories: intersection of the stable invariant manifolds of L_3 with the Moon's surface.

- To study the **sensitivity** of these trajectories we modify some of them:
  - **Mantain** their initial **positions** x and y, as well as the initial **time**, *solar phase* $\vartheta = \omega_s t$.
  - **Modify** their initial **velocity modules** and **angle directions** of the velocity vector, such that a mesh of 10^6 initial conditions is swept.
  - **Analyse the destination**.

Lunar meteorites

Origin of these trajectories: intersection of the stable invariant manifolds of L_3 with the Moon's surface.

- To study the **sensitivity** of these trajectories we modify some of them:
  - **Mantain** their initial **positions** x and y, as well as the initial **time**, *solar phase* $\vartheta = \omega_s t$.
  - **Modify** their initial **velocity modules** and **angle directions** of the velocity vector, such that a mesh of 10^6 initial conditions is swept.
  - **Analyse the destination**.

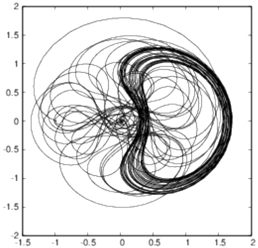

xy-plane (adim units)

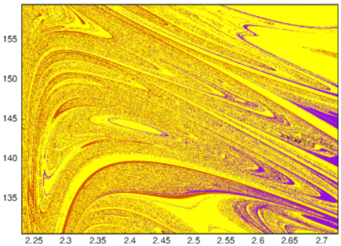

|v| (km/s), angle dir. (degrees)

Color	(**fate**):
Purple	(Earth)
Red	(Moon)
Yellow	(leaving the system)
Black	(neither)

Transport in a realistic model

Bicircular Problem dependence on the time allows the conversion to a realistic model **keeping the information of the relative positions of the Earth, Moon and Sun**.

Transport in a realistic model

Bicircular Problem dependence on the time allows the conversion to a realistic model **keeping the information of the relative positions of the Earth, Moon and Sun**.

Change of coord. and time between models

Transport in a realistic model

Bicircular Problem dependence on the time allows the conversion to a realistic model **keeping the information of the relative positions of the Earth, Moon and Sun**.

Change of coord. and time between models

Time: In the BCP at $t = 0$ or $t = N_T T$ ($N_T \in \mathbb{Z}$), the positions of the Earth, the Moon and the Sun correspond to a **lunar eclipse**, $T_{ECLIPSE}$ in Julian days.

$\rightarrow$ any $t \neq 0$ corresponds to some days before or after the eclipse.

Transport in a realistic model

Bicircular Problem dependence on the time allows the conversion to a realistic model **keeping the information of the relative positions of the Earth, Moon and Sun**.

Change of coord. and time between models

Time: In the BCP at $t = 0$ or $t = N_T T$ ($N_T \in \mathbb{Z}$), the positions of the Earth, the Moon and the Sun correspond to a **lunar eclipse**, $T_{ECLIPSE}$ in Julian days.

$\rightarrow$ any $t \neq 0$ corresponds to some days before or after the eclipse.

Coordinates: The conversion to the **ecliptical system** with the origin in the Solar System centre of mass involves the coordinates of Earth, Moon and their barycentre **at that real time**.

$\rightarrow$ we take the coordinates of Earth, Moon and their barycentre from **JPL database** (Jet Propulsion Laboratory).

Lunar meteorites

Objective: to check the results obtained with the Bicircular model for the lunar meteorites in a more realistic model.

- Apply the **change of coordinates and time to each initial condition** in our adimensional system to translate them to the ecliptic system.

Lunar meteorites

Objective: to check the results obtained with the Bicircular model for the lunar meteorites in a more realistic model.

- Apply the **change of coordinates and time to each initial condition** in our adimensional system to translate them to the ecliptic system.
- Each initial condition is **integrated in a N-body problem** (Earth, Moon, Sun and planets).

Lunar meteorites

Objective: to check the results obtained with the Bicircular model for the lunar meteorites in a more realistic model.

- Apply the **change of coordinates and time to each initial condition** in our adimensional system to translate them to the ecliptic system.
- Each initial condition is **integrated in a N-body problem** (Earth, Moon, Sun and planets).
- Positions and velocities of the massive bodies are obtained from the **JPL ephemeris** DE405 at the right time.

Lunar meteorites

Objective: to check the results obtained with the Bicircular model for the lunar meteorites in a more realistic model.

- Apply the **change of coordinates and time to each initial condition** in our adimensional system to translate them to the ecliptic system.
- Each initial condition is **integrated in a N-body problem** (Earth, Moon, Sun and planets).
- Positions and velocities of the massive bodies are obtained from the **JPL ephemeris** DE405 at the right time.
- **Analyse destination**.

Lunar meteorites

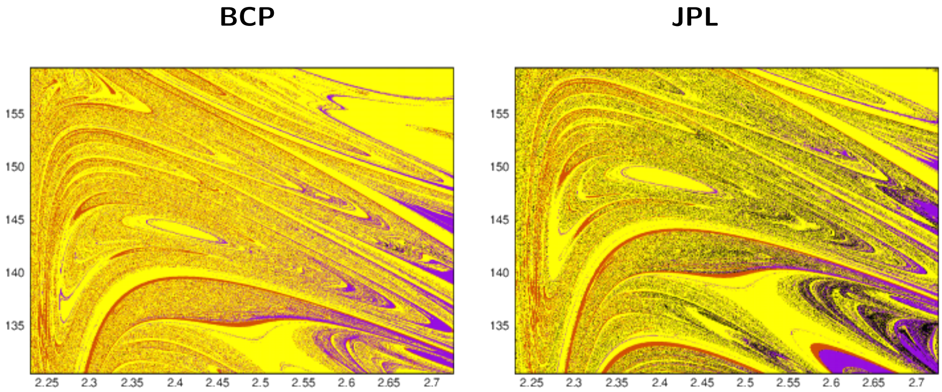

Horizontal axis: $|v|$ (km/s). Vertical axis: angle dir. (degrees).

Color (fate): Purple (Earth), Red (Moon), Yellow (leaving the system), Black (neither).

Capture of an asteroid

Idea is to trap the asteroid in the vicinity of L_3 through the stable invariant manifolds of the invariant curves

Advantages of using L_3: $\begin{cases} \text{Very cheap station keeping} \\ \text{Gateway towards other regions} \end{cases}$

Capture of an asteroid

Idea is to trap the asteroid in the vicinity of L_3 through the stable invariant manifolds of the invariant curves

Advantages of using L_3: $\left\{ \begin{array}{l} \text{Very cheap station keeping} \\ \text{Gateway towards other regions} \end{array} \right.$

Strategy:

Capture of an asteroid

Idea is to trap the asteroid in the vicinity of L_3 through the stable invariant manifolds of the invariant curves

Advantages of using L_3: $\begin{cases} \text{Very cheap station keeping} \\ \text{Gateway towards other regions} \end{cases}$

Strategy:

- Translate the coordinates of a real asteroid to the BCP reference frame at the right time.
  $\rightarrow$ change of coordinates.

Capture of an asteroid

Idea is to trap the asteroid in the vicinity of L_3 through the stable invariant manifolds of the invariant curves

Advantages of using L_3: $\begin{cases} \text{Very cheap station keeping} \\ \text{Gateway towards other regions} \end{cases}$

Strategy:

- Translate the coordinates of a <u>real asteroid</u> to the BCP reference frame at the right time.
  $\rightarrow$ change of coordinates.
- Globalize <u>backward in time</u> the trajectories on the stable invariant manifolds of L_3 to compare them with the positions of the asteroid. $\rightarrow$ it must be done at the same time.

Capture of an asteroid

Idea is to trap the asteroid in the vicinity of L_3 through the stable invariant manifolds of the invariant curves

Advantages of using L_3: $\begin{cases} \text{Very cheap station keeping} \\ \text{Gateway towards other regions} \end{cases}$

Strategy:

- Translate the coordinates of a real asteroid to the BCP reference frame at the right time. $\to$ change of coordinates.
- Globalize backward in time the trajectories on the stable invariant manifolds of L_3 to compare them with the positions of the asteroid. $\to$ it must be done at the same time.
- Colour the FC according to the distance to the asteroid to identify the one that lies on the position of the asteroid. $\to$ high order approximation of the manifolds is needed.

Capture of an asteroid

Idea is to trap the asteroid in the vicinity of L_3 through the stable invariant manifolds of the invariant curves

Advantages of using L_3: $\begin{cases} \text{Very cheap station keeping} \\ \text{Gateway towards other regions} \end{cases}$

Strategy:

- Translate the coordinates of a real asteroid to the BCP reference frame at the right time. $\rightarrow$ change of coordinates.
- Globalize backward in time the trajectories on the stable invariant manifolds of L_3 to compare them with the positions of the asteroid. $\rightarrow$ it must be done at the same time.
- Colour the FC according to the distance to the asteroid to identify the one that lies on the position of the asteroid. $\rightarrow$ high order approximation of the manifolds is needed.
- The difference in velocities gives the cost of the maneuver. $\rightarrow$ Δv (m/s).

High order parametrization of hyperbolic invariant manifolds

Invariant curve φ in a Poincaré temporal map P, $P(\varphi(\theta)) = \varphi(\theta + \omega)$

The h.o. **parametrization** of the manifolds associated to φ depends on two parameters, $\theta \in \mathbb{T}^1$ and $\sigma \in \mathbb{R}$, and can be written as a Taylor-Fourier expansion:

$$W(\theta, \sigma) = a_0(\theta) + a_1(\theta)\sigma + \sum_{k \geq 2} a_k(\theta)\sigma^k,$$

that must satisfy **invariance condition**: $P(W(\theta, \sigma)) = W(\theta + \omega, \lambda\sigma)$,

- We solve this equation order by order, for which we need the derivatives of the map.

• The **Jet transport** (JT) technique allows to compute high order derivatives of the flow of an ODE with respect to initial data and/or parameters, based on using automatic differentiation on a numerical integration of ODEs. → In [1], authors develop an integrator based on JT for **Poincaré maps**.

---

[1] J. Gimeno, À. Jorba, M. Jorba-Cuscó, N. Miguel, and M. Zou. Preprint, 2021

Parametrization of the stable FC

$$z(\theta,\tau)=\sum_{k=0}^{K} a_k^s(\theta)((1+\tau(1/\lambda_s-1))\sigma)^k,$$

where $z(\theta,\tau)\in\mathbb{R}^n$ and $\tau\in[0,1]$. When $\tau=0$, $z(\theta,\tau)$ parametrizes the lower curve, $W_K^s(\theta,\sigma_0)$, and when $\tau=1$ it parametrizes the upper curve, $W_K^s(\theta,\lambda_s^{-1}\sigma_0)$.

- K is the maximum order so that the error is of order σ^{K+1}.
- We considered is $K=16$.
- Compute the trajectory such that $F(\theta,\tau)=\{x(\theta,\tau),y(\theta,\tau)\}_{t_f}-\{x_{asteroid},y_{asteroid}\}\equiv 0$.

Results for 2006 RH120

2006 RH120 is a Near Earth Asteroid (NEA) that comes close to the Earth from time to time.

$\rightarrow$ We analyse the capture in its approach of 2006,
studying different epochs from April 2006 to May 2007.

Here we only present one of them.

Results for 2006 RH120. For 2006-Jun-25 (t=mod(T/2) in BCP)

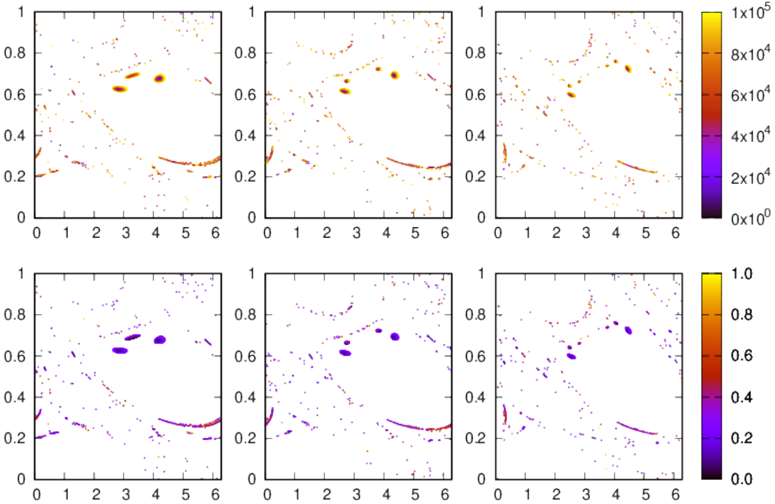

FCs of tori **at distances from L_3 between** 0.02159 **and** 0.03947. First row, FCs coloured according to the distance to the asteroid in km at position $x = -2.38595, y = -3.06967$. Second row, the same FCs coloured according to the instantaneous Δv in km/s.

Results for 2006 RH120. For 2006-Jun-25 (t=mod(T/2) in BCP)

	Min 1		
dist to L_3	θ	τ	Δv (m/s)
0.02159	2.856	0.626	19.398
0.02738	2.693	0.615	19.386
0.03947	2.555	0.597	19.338
	Min 2		
dist to L_3	θ	τ	Δv (m/s)
0.02159	4.224	0.678	19.338
0.02738	4.373	0.693	19.293
0.03947	4.472	0.725	19.176

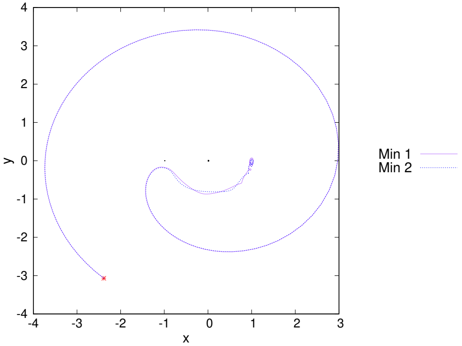

Left, values of the initial conditions in the FCs that after N_T BCP periods lay on the position of the asteroid at June 25, 2006 and the Δv required for each of them. Right, **simulation of the capture** of the asteroid by the trajectories in the two bigger minimum distance areas on the third FC when applying the obtained Δv.

Conclusions

- The role of L_3 equilibrium point in the planar Earth-Moon system under the perturbation of the Sun has been studied.
- We have **numerically computed** and **analysed**:
  - The family of invariant tori that emanates from L_3 and their linear behaviour.
  - The linear and high order approximation of the hyperbolic invariant manifolds.
  - Connections between stable and unstable manifolds of L_3 tori.
- Special attention was paid to two **astrodynamical applications**:
- The behaviour of lunar meteorites found on the Earth surface.
  - Results checked in a realistic model.
- The possibilities of capture of an asteroid in the BCP.

Conclusions

- The role of L_3 equilibrium point in the planar Earth-Moon system under the perturbation of the Sun has been studied.
- We have **numerically computed** and **analysed**:
  - The family of invariant tori that emanates from L_3 and their linear behaviour.
  - The linear and high order approximation of the hyperbolic invariant manifolds.
  - Connections between stable and unstable manifolds of L_3 tori.
- Special attention was paid to two **astrodynamical applications**:
- The behaviour of lunar meteorites found on the Earth surface.
  - Results checked in a realistic model.
- The possibilities of capture of an asteroid in the BCP.

Thank you for your attention!

Variedades invariantes y transporte en un sistema Tierra-Luna perturbado por el Sol

À. Jorba, B. Nicolás

Ddays, Lleida, 9 de Septiembre del 2021